Feasibility of a Vascular-Specific Super Resolution Ultrasound Algorithm for Prostate Cancer Imaging

FEASIBILITY OF A VASCULAR-SPECIFIC SUPER RESOLUTION ULTRASOUND ALGORITHM FOR PROSTATE CANCER IMAGING

M. Butler[1], G. Papageorgiou[1], A. Mobberley[1], E. Kanoulas[2], N. Leslie[1], J. Keanie[3], K. Gallagher[3], D. Good[3], A. McNeill[3], W. Lu[1], V. Sboros[1]

[1]Heriot-Watt University, Institute of Biological Chemistry, Biophysics and Bioengineering, EPS, Edinburgh, UK
[2]Janssen Pharmaceuticals R & D, High Wycombe, UK
[3]NHS Lothian, Western General Hospital, Edinburgh, UK

ABSTRACT

Contrast agents in ultrasound imaging are gas filled microbubbles which remain within the vascular network. Super-resolution ultrasound imaging (SRUI) can be achieved by tracking the contrast agent echoes and creating maps depicting the vasculature. In this work, a new vascular-specific SRUI tracking algorithm was developed using a synthetic network and applied to contrast enhanced ultrasound video data collected from patients with known prostate cancer. The output from SRUI was compared to post-operative pathology assessment of the same prostates. Vascular dynamics in regions of known cancer were evaluated and compared to regions of normal prostate structure. Faster and higher volume blood flow was found at locations associated with significant prostate cancer.

Index Terms— prostate cancer, super resolution ultrasound, microbubbles, vascular networks, abnormal blood flow

1. INTRODUCTION

Super resolution ultrasound imaging (SRUI) based on detection, localization and tracking of ultrasound microbubble contrast agents has been shown to have significant potential as a diagnostic imaging tool [1-3]. The tracking of microbubbles within the circulation can provide information on both the vascular microstructure and dynamics. One potential application is imaging of prostate cancer. Diagnosis of prostate cancer is challenging and currently has no reliable method of screening. The assessment of prostate specific antigen (PSA) does not provide adequate diagnostic sensitivity as this gradually changes over time in many normal prostates [4]. MRI imaging has been introduced to triage prostate patients for biopsy, however, a) clinically significant cancers are still missed and b) patients with clinically insignificant cancers undertake unnecessary biopsies [5]. As prostate cancer concerns a large population, a cost-effective imaging tool that can improve diagnostic accuracy and thus patient management is much needed. The objective of the work described here was to investigate the feasibility of SRUI in patients with known prostate cancer as well as seek associations with neo-vascular domains, their patterns and blood flow dynamics as represented in SRUI maps.

2. MATERIALS AND METHODS

2.1. In Silico Methods

Algorithms developed for SRUI were initially assessed on synthetic and in vivo, pre-clinical data [3]. Synthetic assessments included creating a fluid flow network where microbubbles within the vascular network were simulated. The synthetic vascular network comprised vessels ranging 0.5-2 mm in diameter. The simulated data applied was based on real ultrasound data, the process used is described in Kanoulas et al (2019). The coordinates of the simulated data particles were recorded and used to create a video of synthetic data through a theoretical flow network. The first SRUI algorithm applied utilized a nearest neighbor (NN) approach [3] where detected microbubble echoes (detections) which were close together in consecutive image frames were linked to create tracks. A second SRUI algorithm was developed to emulate vessel-like motion (VM) using only forward travel of detections. Therefore, rejecting any microbubble links which would be outside of a vessel. The accuracy of the detection, localization and tracking of the microbubbles using both algorithms was assessed in the synthetic network.

2.2. Clinical Methods

The algorithms were then applied to clinical ultrasound data. Imaging was undertaken using a Philips iU22 scanner (Philips Medical Imaging, Seattle, WA, USA) with a C3-10V intracavity probe running in contrast specific mode. Luminity® perflutren lipid microbubbles (Lantheus, Bedford, MA, USA) was administered by gravity infusion, at a dose of 2.6mL activated Luminity® in 100 mL saline and a steady rate of 250 ± 20 mL/hr. With the transducer secured in

a single location, a 3-4 minute video of contrast infusion was saved and later processed offline. Initially the saved video data were corrected for motion due to respiration [6]. The image frames were cropped around the prostate boundary and the algorithms were applied to the saved video data thus producing SRUI dynamic maps of the prostate vasculature. After ultrasound scanning, each patient had radical prostatectomy, the removed prostate was processed and inspected by pathology. In addition to the post-op pathology, pre-op clinical information including MRI reports and images, PSA levels and systematic biopsy results were available to include in analysis. Of the first 10 cases scanned for the study two were excluded due to poor data quality.

3. RESULTS AND DUSCUSSION

3.1. In silico tracking results

The emphasis here was to develop a SRUI tracking algorithm that generated robust maps in order to depict all vessels correctly. The synthetic data showed that the SRUI maps were a true reflection of the original network structure (Fig.1). False tracks, were generated with the NN algorithm when vessels were close to each other particularly at bifurcations, resulting in erroneous vessels as well as loss in resolution by showing increased bifurcation thickness (Fig. 1c). The newly developed VM tracking method (Fig. 2d) minimized the errors between vessels and displayed improved resolution. The VM algorithm reduced false tracks within the whole network to below 5% (Fig.2d), which is a significant improvement compared to around 20% false tracks of the original NN algorithm (fig.2c). This also resulted in a 25% decrease in the total number of paired` microbubbles. The reduction in false tracks reduced the likelihood of generating artefactual vessels and ensured the creation of reliable, well defined structural maps, improved velocity measurement in each vessel that could be used for further processing and comparisons with ground truth data.

3.2. An example prostate comparison between SRUI, MRI and pathology

The VM algorithm was applied to clinical data and the output from one example is shown in Figure 2. Fig 2 a-d are the multiparametric (mp) MRI images from a case where prostate cancer was suspected. The arrowed region in Fig. 2a, the T2 weighted MRI image, indicates a hypointense region which corresponds to a region of increased intensity in (b) which is the dynamic contrast MRI. Similar, although more subtle, hypo and hyper intense regions are seen in the diffusion MRI ADC and B-1400 images, (c), (d) respectively. These parameters indicate that there is a vascularized lesion in the anterior right prostate (top left of image) in the apex of the prostate [7]. SRUI maps are shown in Fig. 2f-h representing velocity, number of tracks (number of tracks created through each pixel) and blood flow respectively. Blood flow is the product of velocity and track number thus enhances regions of faster and higher volume. On the patient right side (image left) there is a clear band where there is faster and higher volume blood flow as well as a similar central band. In contrast the left side (image right) shows slower and lower volume blood flow.

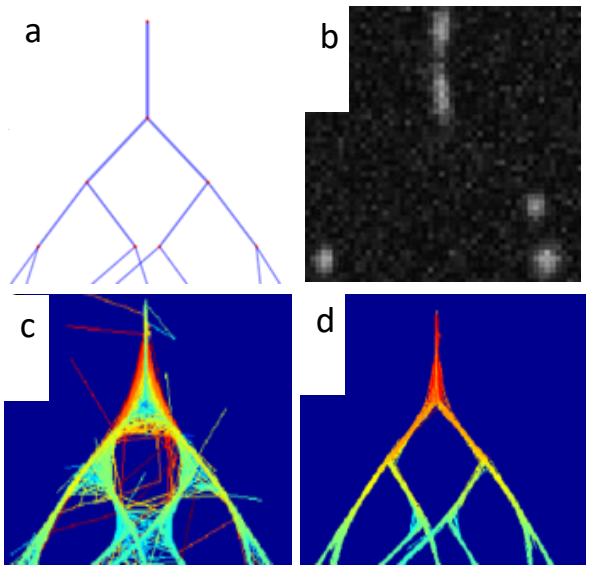

Fig. 1. Super resolution imaging within a synthetic network, a) section of the network showing linked vessels, decreasing in length and diameter, b) single frame of ultrasound data from synthetic contrast ultrasound data created within the same region of the network, c) super resolution map created from processing a simulated image sequence collected within the synthetic network using the NN tracking. False tracks between neighboring vessels were created especially when the vessels were close together d) super resolution map with the new VM linking. Significantly fewer false tracks are shown compared to c) as seen by the presence of well-defined vessels and bifurcations.

The SRUI maps were compared to the post-op pathology slice (Fig.2i) closest to the apex, where the tumor was marked by the pathologist. The locations of the areas of increased bloodflow in the SRUI maps are very close to or within the pathology marked boundaries. In addition, there is a posterior lesion (bottom of image, arrowed on Fig. 2i) which was not detected on MRI (Fig. 2 a-d). This region is associated with an increase in blood flow in SRUI (Fig. 2 f-h (arrowed in h)) suggesting that vascular structure and dynamics are important in prostate cancer identification, with parts of lesions comprising higher blood velocities and volume, likely to be due to angiogenesis. It is known that angiogenesis is linked to prostate cancer tumours and the location of the neo-

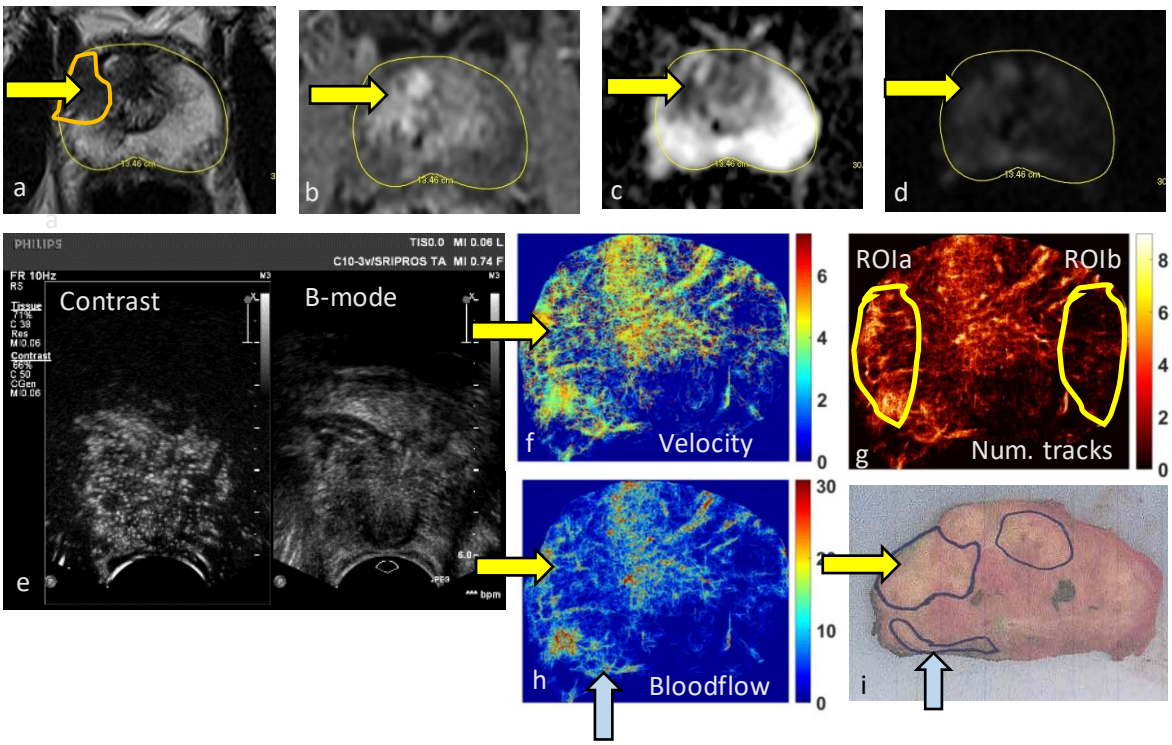

Figure 2: Example case of prostate cancer (towards apex of prostate) a, b, c, d are mp-MRI images in the order T2-weighted image with suspect region marked and arrowed, Dynamic contrast, ADC and B1400 (both part of a diffusion MRI imaging sequence). e) Example ultrasound image frame (left side contrast, right side B-Mode) f,g,h super resolution images from contrast ultrasound video data representing velocity (mm/s), number of tracks and bloodflow (product of track number and velocity), yellow marked regions on track number maps are size-matched regions of interest where the number of tracks and velocity were compared: median velocity of ROIa was 3.61 mm/s (quartiles 2.8, 4.3) compared to ROIb 2.79 mm/s (quartiles 1.6, 4.0) ($p<0.01$) with the total number of tracks created in each being 8149 and 3628 respectively, i) post-operative pathology of the same prostate at a closely matched location within the prostate, with regions of cancer, determined by histological evaluation, marked.

vasculature changes over time [8], however blood flow volume and blood velocity is not exclusive to cancer, further assessment of the vessel structures may be able to provide more information on the cellular structures in the imaging region.

In order to obtain general values for large sections of prostate regions of interest (ROI) were selected on both sides of the prostate (approximate ROIs marked on the track number map in Fig. 2 g). In the example detailed here, the median velocity on the left side of the prostate (image right) was 2.79 mm/s (1st and 3rd quartiles 1.6, 4.0, number of tracks 3628) compared to 3.61 mm/s (1st and 3rd quartiles 2.8, 4.3 number of tracks 8149) ($p<0.01$) on the right side of the prostate (image left). The ROIs were the same size in each case. The analysis also showed that there were more tracks created on the right side of the prostate where most of the cancer was identified.

3.3. Clinical Summary and overview of prostate structure

Of the 8 datasets available for assessment each one showed regions of increased blood flow at locations corresponding to cancer identified on post-op pathology compared to the rest of the prostate. In addition to areas associated with clinically significant cancer (Gleason 3+4=7) some regions within the prostate are generally more vascularized than others such as the transition zone in older patients. The SRUI processing provides micrometric resolution maps of vascular networks within the prostate which provides more information than typical parameters calculated from contrast enhanced ultrasound such as mean transit time or peak intensity [9]. In addition to high flow and vascular density, in some cases SRUI reveals complex structure and dynamic features that are difficult to detect otherwise, these can also be dependent on location within the prostate.

In the area surrounding the urethra (usually centrally located within the prostate) there are large blood vessels therefore increased blood flow. It would be valuable to be able to distinguish between hyper-blood flow regions in normal prostate tissue, inflamed prostate tissue and regions of clinically significant cancer.

A more in-depth assessment of the parameters calculated from SRUI processing may provide more specific information to allow distinction between cancer and normal prostate regions as well as distinguish between other conditions found within prostate such as prostatitis, or benign prostatic hyperplasia (BPH).

4. CONCLUSION

Synthetic vessel networks can be used to assess the performance of algorithms designed to detect and track microbubbles within vascular networks. When applied to clinical cases of known prostate cancer it was seen that increased blood flow by both faster blood flow and more tracks were present in regions of confirmed cancer by comparison of SRUI maps with post-operative pathology. All cancer regions from 8 cases had regions of increased blood flow at the pathology confirmed cancer location. SRUI maps represent the vascular network and their dynamics within the prostate and have the potential to provide valuable information on both the structure and flow dynamics of the prostate. Future work includes more detailed assessment of the vascular structure and blood flow dynamics to differentiate significant cancer from benign/normal prostate tissue and inflamed prostate tissue.

5. COMPLIANCE WITH ETHICAL STANDARDS

Full ethical approval was granted to allow contrast enhanced ultrasound scanning of patients with known prostate cancer at the Western General Hospital, Edinburgh, UK (ISRCTN 62147629).

6. ACKNOWLEDGMENTS

This work was funded by the Chief Scientist Office (CSO), Scotland, CS/18/40. The authors would like to acknowledge Research Grant support from Lantheus, Bedford, MA, USA in the form of Luminity ® perflutren lipid microbubble agent used for the clinical work presented here.

In addition, we are very grateful to Research Nurses Marion McRury and Athena Oddy as well as Linda Taylor and the theatre teams, anesthetists and pathologists at the Western General Hospital, Edinburgh, UK for all the help and guidance given when acquiring the clinical data.

7. REFERENCES

[1] Christensen-Jeffries, K., et al., In vivo acoustic super-resolution and super-resolved velocity mapping using microbubbles. IEEE Trans Med Imaging, 2015. 34(2): p. 433-40.

[2] Christensen-Jeffries, K., et al., Super-resolution Ultrasound Imaging. Ultrasound in Medicine and Biology, 2020. 46(4): p. 865-891.

[3] Kanoulas, E., et al., Super-Resolution Contrast-Enhanced Ultrasound Methodology for the Identification of In Vivo Vascular Dynamics in 2D. 2019.

[4] Berges, R. and M. Oelke, Age-stratified normal values for prostate volume, PSA, maximum urinary flow rate, IPSS, and other LUTS/BPH indicators in the German male community-dwelling population aged 50 years or older. World J Urol, 2011. 29(2): p. 171-8.

[5] Waldén, M., et al., A Head-to-head Comparison of Prostate Cancer Diagnostic Strategies Using the Stockholm3 Test, Magnetic Resonance Imaging, and Swedish National Guidelines: Results from a Prospective Population-based Screening Study. European Urology Open Science, 2022. 38: p. 32-39.

[6] Perperidis, A., et al. Automatic dissociation between microvasculature and larger vessels for ultrasound contrast imaging. in 2014 36th Annual International Conference of the IEEE Engineering in Medicine and Biology Society. 2014.

[7] Ahmed, H.U., et al., Diagnostic accuracy of multi-parametric MRI and TRUS biopsy in prostate cancer (PROMIS): a paired validating confirmatory study. The Lancet, 2017. 389(10071): p. 815-822.

[8] Russo, G., et al., Angiogenesis in prostate cancer: onset, progression and imaging. BJU Int, 2012. 110(11 Pt C): p. E794-808.

[9] Butler, M., et al., Differentiation of Vascular Characteristics Using Contrast-Enhanced Ultrasound Imaging. Ultrasound in Medicine and Biology, 2019. 45(9): p. 2444-2455.